Feasibility study of layer separation using 2D patterned internal laser damage in silicon

Yuan Yao[1,2†], Andrea Vergara[1*], Zhengnan Tang[1] and Shuji Tanaka[1]

[1]*Department of Robotics, Tohoku University, Sendai 980-8579, Japan*

[2]*School of Mechanical and Aerospace Engineering, Jilin University, Changchun 130022, China*

[†]This author was an exchange student in Tohoku University.

*E-mail: vergara@tohoku.ac.jp

Laser lift-off (LLO) technology is widely used to separate ultra-thin electronic devices and in advanced packaging but typically relies on a specialized laser-responsive layer, adding complexity. This paper presents an innovative take on stealth dicing by using a pulse laser in a two-dimensional plane to create a separation interface without requiring a special layer, thus simplifying the fabrication process. The relationship between shear strength and laser ablation parameters was analyzed through shear force tests, with the modified layer morphology also examined. Shear strength for separation ranged from 200 to 20 MPa, with lower values achieved by reducing scanning pitch, increasing laser power, or enlarging the separated area. These findings highlight the potential of 2D stealth dicing as an LLO technique for ultra-thin devices.

1. Introduction

Electronic devices are gradually transitioning from flat, rigid components to curved or flexible ones. The growing demand for wearable devices has accelerated the development of flexible transducers[1-3]. One direct approach is to use naturally soft materials, such as polymers and fluids[4]. However, this often results in sacrificing performance. As a result, various techniques have been developed to transform or transfer rigid microdevices onto flexible substrates while retaining their high performance[5-9]. Many of these techniques rely on etching sacrificial layers, but this approach is challenging to apply to piezoelectric MEMS devices, which have gained popularity due to their compactness, low voltage requirements, and ultra-low energy consumption. Several examples of thin-film piezoelectric layers grown on Si or other rigid substrates and then transferred to flexible substrates can be found in the literature[10-13]. The major challenge with this approach is the risk of delamination due to poor adhesion to the target substrate, underscoring the need for a more reliable method.

Recently, laser lift-off (LLO) technology has gained significant attention in the development of ultra-thin electronic devices due to its non-contact processing advantage[14]. It has been widely used in micro-LED fabrication and advanced packaging for electronic components[15-21], with companies like EVG[22], Disco[23], and TEL[24] releasing their own LLO technologies. Current LLO methods typically require a laser-responsive layer that facilitates separation when ablated. This method, while effective, introduces limitations such as additional fabrication steps and material constraints. In the case of piezoelectric devices, the laser-responsive layer typically cannot withstand the high temperatures required for piezoelectric thin-film deposition.

To overcome these challenges, we explored stealth dicing (SD)[25-28], an advanced laser-based technique that ablates substrates at arbitrary depths without needing a special absorbing layer. Unlike typical LLO technology, SD uses a high numerical aperture lens to focus the laser pulse into a condensed point, concentrating the laser energy. As a result, even when the material is transparent to the laser, the laser can interact with the material inside at the focal point by two photon absorption, creating voids, cracks, or other damages. Also, rapid temperature increase generates an “SD layer” through a thermal shockwave[29-31]. As the laser scans, the SD layer forms continuously, and interactions between these layers induce cracks in the material, greatly reducing the substrate's mechanical strength.

However, SD is conventionally used to dice chips into smaller pieces. In this study, the pulsed laser was used to “cut” closely spaced lines within the Si substrate, creating a weakened plane that allows easy separation by applying shear stress[32]. This method could

greatly simplify the transfer of piezoelectric devices to flexible substrates while preserving the integrity of the active device layers. For example, Figure 1 illustrates the conceptual fabrication process of a high-performance flexible pMUT array. In this paper, shear force tests were conducted to evaluate the mechanical strength under different laser ablation parameters, and the morphology of the SD layer after laser ablation was analyzed using optical and scanning electron microscopy (SEM).

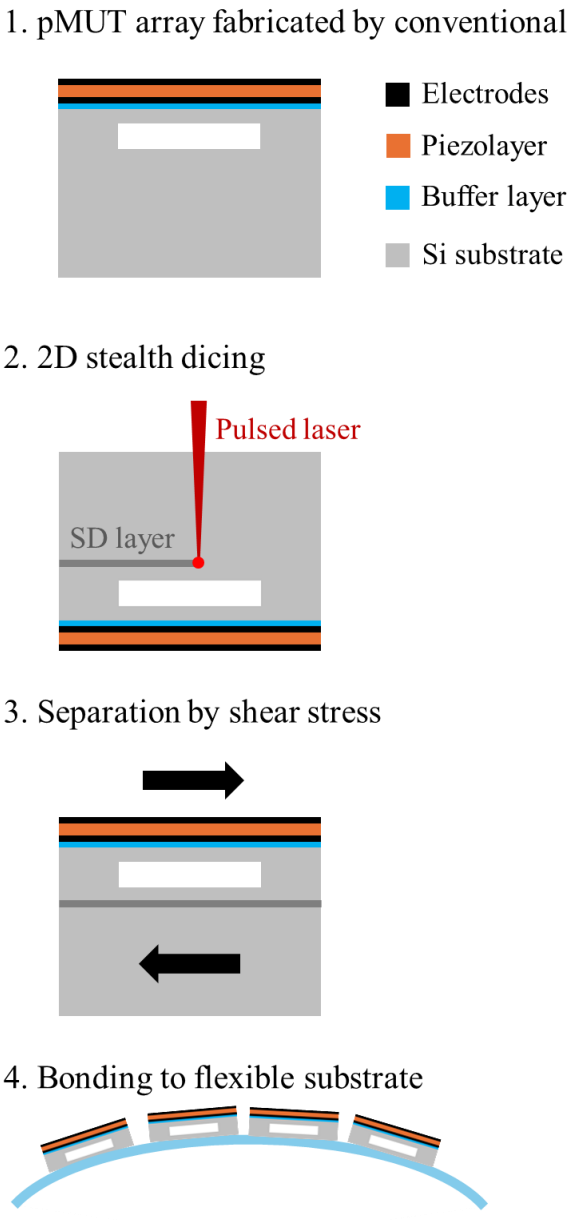

Fig. 1. Conceptual fabrication process of flexible pMUT array for wearable devices. The initial fabrication of the pMUT is done by conventional MEMS processes, then the proposed two-dimensional stealth dicing layer is cut to generate a weakened plane at an arbitrary height, which is later separated by the application of shear stress, and the resulting ultra-thin pMUTs are bonded to a flexible substrate.

2. Experimental methods

Figure 2 illustrates the fabrication process and experiment flow of the test samples beginning with a plain silicon wafer. The first step involved using Deep Reactive Ion Etching (DRIE) (MUC-21 ASE-SRE, Sumitomo Precision Products Co. Ltd., Japan) to form the desired square shapes. Subsequently, a pulsed fiber laser (1064 nm wavelength, pulse width 200 ns, max. power 1.2 W, repetition frequency 20 – 500 kHz, model SP-12P-HS-B-B-B-B, SPI Lasers, UK) was employed to induce internal damage beneath the smooth Si surface along a two-dimensional patterned path. The configuration of the laser dicer equipment used is shown in Figure 3. The laser scanning pattern was a square grid with a scanning pitch ranging from 5 to 15 μm. Finally, shear force tests were conducted to evaluate the separation strength.

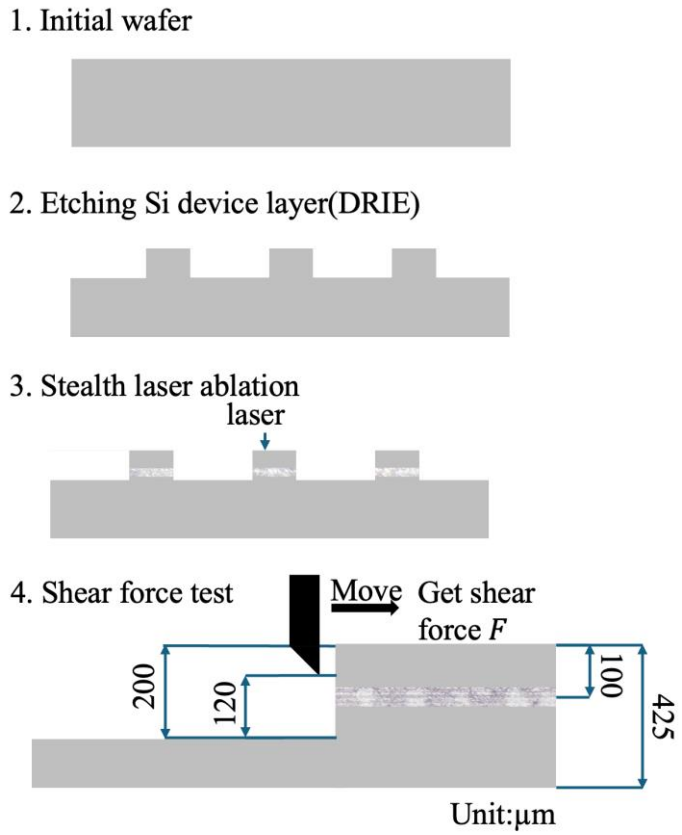

Fig. 2. Experiment flow. (1) Initial Si wafer (1 0 0) of 400 μm thickness. (2) Fabrication of square-shaped structures by DRIE. (3) Stealth laser ablation at approximately the foot of the structure to induce easy separation. (4) Separation using a shear force measurement equipment.

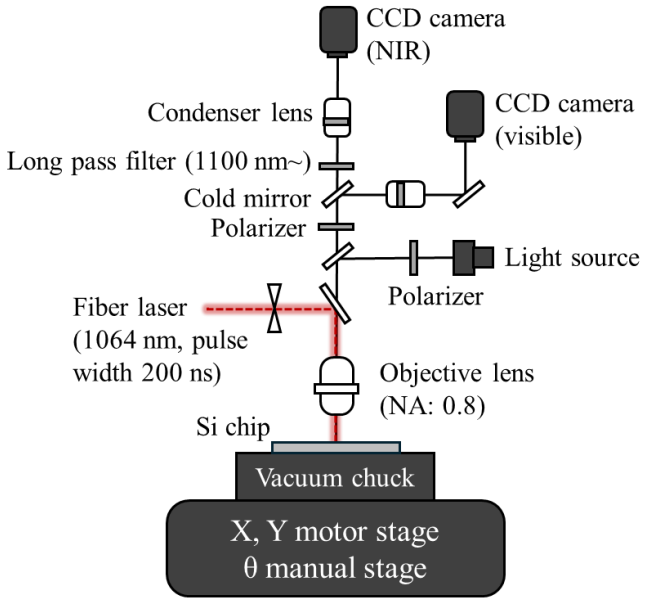

Fig. 3. Configuration of laser dicer equipment.

Figure 4 presents a series of photographs during the actual experimental process. Figure 4(a) shows the mask design used for lithography and DRIE. A thick wall was included to prevent the formation of black silicon during the DRIE process, with the square pattern sizes ranging from 100 to 500 μm, as larger sizes tend to fracture the Si substrate during shear force test. Figure 4(b) depicts the wafer after lithography, which has an orientation of <100> and a thickness of 400±15 μm. The photoresist used was PMER P-LA 900 PM (Tokyo Ohka Kogyo, Japan), which was thick enough to avoid its partial removal during the DRIE process. Figure 4(c) shows the wafer after DRIE and cleaning. The average height of the DRIE etching was around 200 μm. Resist removal was performed using acetone and Piranha solution (98% sulfuric acid: hydrogen peroxide = 3:1). Figure 4(d) illustrates the dicing step (DAD3240, DISCO Co., Japan), where the 4-inch wafer was divided into 2×2 cm² dies, as the laser dicer is limited to processing samples of this size. Figure 34e) displays the stealth laser ablation step using the laser dicer, which employs a ×100 IR lens to focus the laser into a very small point, inducing internal damage within the Si. The sample stage moved freely at 2 mm/s in the X-Y plane, guided by points from a CSV file, allowing for customizable laser scanning paths. Figure 4(f) captures the shear force test conducted using a Bonding Force Measurement System (PTR-1101, Rhesca Co. Ltd., Japan), where the shear force, F, required to separate each pattern was measured. After dividing by the pattern size, the shear stress (τ) was calculated, providing crucial data for evaluating mechanical strength and optimizing laser scanning pitches and other processing parameters.

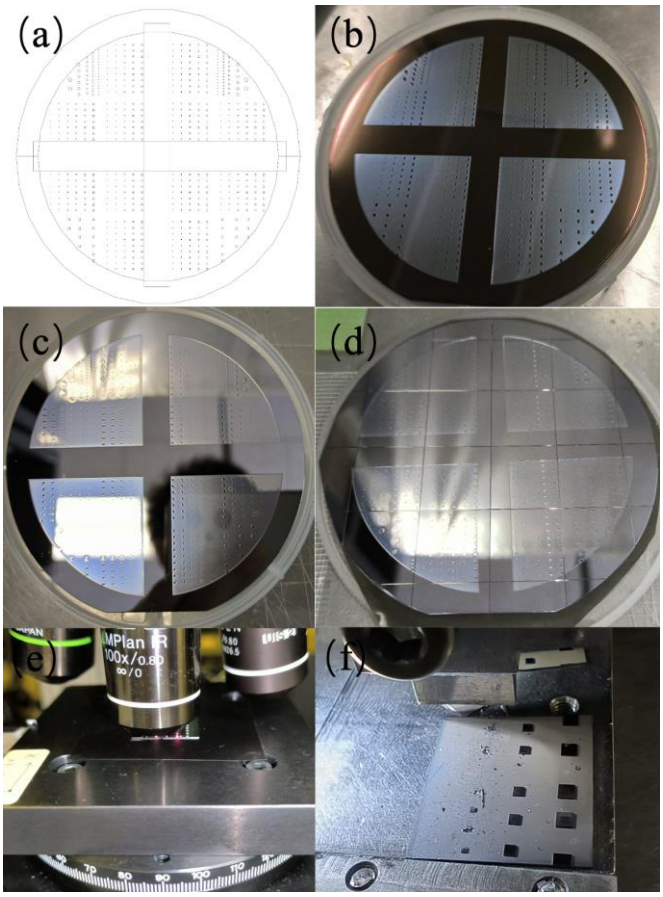

Fig. 4. Photographs of the testing sample (a) Mask design; (b) Lithography; (c) DRIE and cleaning; (d) Dicing; (e) Stealth laser ablation; (f) Shear force test.

A detailed diagram of the shear force test is presented in Figs. 5 and 5. During internal laser ablation, voids with diameters between 1 and 3 μm are created by two photon absorption and high temperatures at the laser focal point, which also generates a thermal shock wave, leading to the formation of the SD layer. As the laser scans, the SD layer continuously forms and interacts, creating internal cracks that significantly reduce the mechanical strength of the material. In the shear force test, by aligning the blade with the SD layer and applying horizontal shear force, the Si above the SD layer can be easily separated.

While the cross-sectional morphology of stealth dicing has been extensively studied[25], [26], [27], [28], [29], [30], the top-view structures have not been reported. Therefore, photographs of the SD layer, substrate, and separated layer were taken and analyzed. During the imaging of the top layer, the sample is typically very small and prone to displacement following the application of shear force. To prevent this, adhesive tape is applied to the surface prior to conducting the shear force test.

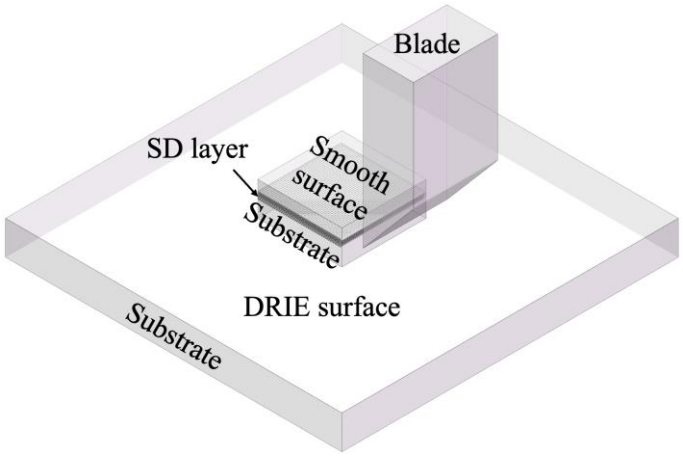

Fig. 5. Isometric diagram of the shear force test.

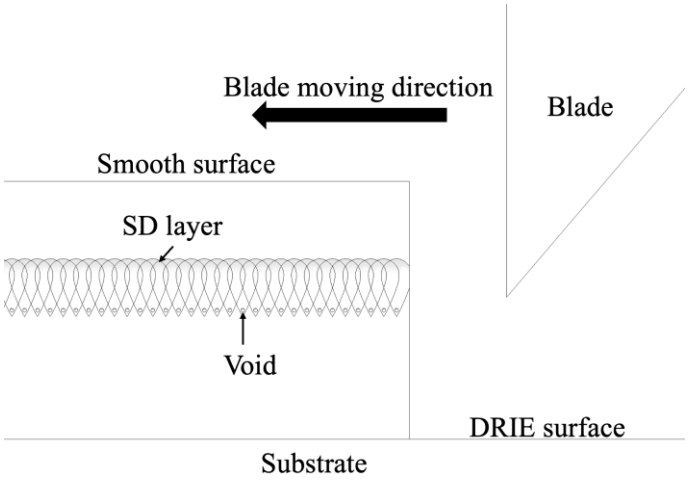

Fig. 6. Magnified cross-section diagram of the shear force test.

3. Results and discussion

3.1 Results

Three parameters have shown distinctive effect in lowering shear strength: laser scanning pitch, laser power and the pattern size. The scanning speed was kept constant at a maximum of 2 mm/s. The combination of parameters used is summarized in Table I. As shown in Fig. 7, the correlations between shear stress (τ), and these parameters are detailed.

Table I. Summary of parameters used in the experiments.

Parameter	Value				
Scanning pitch (μm)	5		10*		15
Laser power	130* (~0.147 W)	150 (~0.17 W)	200 (~0.22 W)	250 (~0.282 W)	300 (~0.339 W)
Pattern size (μm^2)	100×100	200×200	300×300*	400×400	500×500

*Default value when varying other parameters.

Figure 7(a) presents the relationship between shear stress and laser scanning pitch, conducted with a sample size of 300×300 μm² and a laser power of 130. The results indicate a positive correlation between shear stress (τ) and laser scanning pitch. This suggests that a denser laser path facilitates layer separation in Si. However, it also results in a longer processing time during the stealth laser ablation step.

Figure 7(b) is conducted with a laser path pitch of 10 μm and a sample size of 300×300 μm². The shear stress decreases rapidly as laser intensity increases from 130 to 150. The laser intensity can be selected in the controller from 0 to 1000, where 1000 means 100% intensity. In Table 1 the estimated laser power in Watts are included as a reference, though they were not confirmed. Beyond this range, the reduction in shear stress became less pronounced. In practical experiments, laser intensities above 300 are hazardous, while intensities around 100 or lower are insufficient to damage silicon. Therefore, a laser intensity of 150 is recommended.

Figure 7(c) illustrates an experiment conducted with a laser power of 130 and a laser path pitch of 10 μm. The shear stress exhibits a negative correlation with pattern size, suggesting that larger patterns are easier to separate. However, any pattern with a side length greater than 500 μm is likely to cause substrate breakage during shear force test.

Figure 8 presents a selection of optical and scanning electron microscopy (SEM; SU-70, Hitachi, Japan) images of the tested samples. Figure 8(a) illustrates the effect of laser ablation on the smooth Si surface, showing significant morphological changes from left to right. This variation was due to slight height differences in either the sample or the stage, resulting in varied interactions of the SD layer. Figure 8(b) depicts the texture of the SD layer on the substrate after the shear force test, where the top layer has been completely removed, revealing a distinct laser scanning path. Figure 8(c) provides a magnified view of the laser-ablated layer on the substrate after the shear force test, clearly showing the presence of voids. Figure 8(d) shows the separated top layer, which was collected during the shear test using tape. The border of this layer is slightly damaged, but the central part remained intact, demonstrating the theoretical feasibility of developing a separation technology for transferring ultra-thin electronic devices.

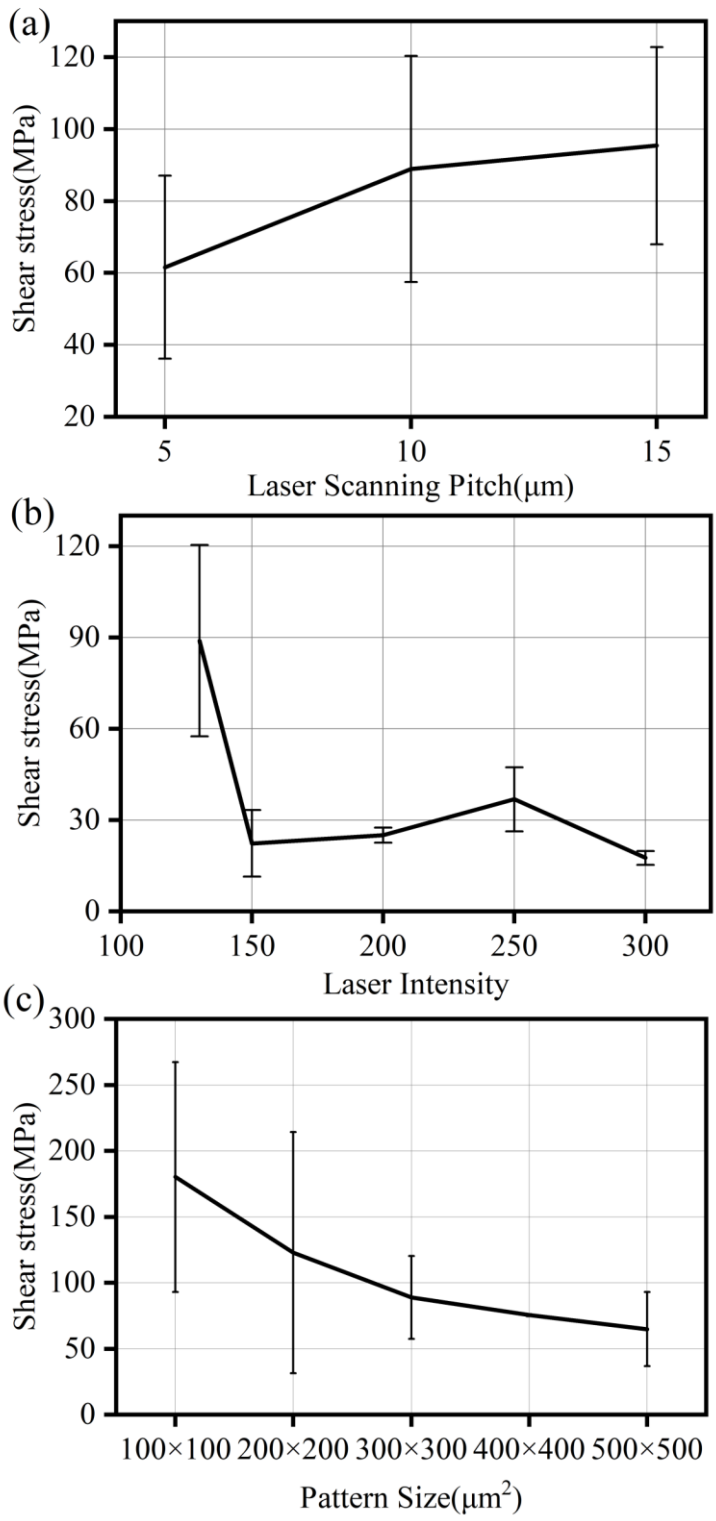

Fig. 7. Relationship between the shear stress and (a) laser scanning pitch (μm); (b) laser intensity (percentage); (c) pattern sizes (μm^2).

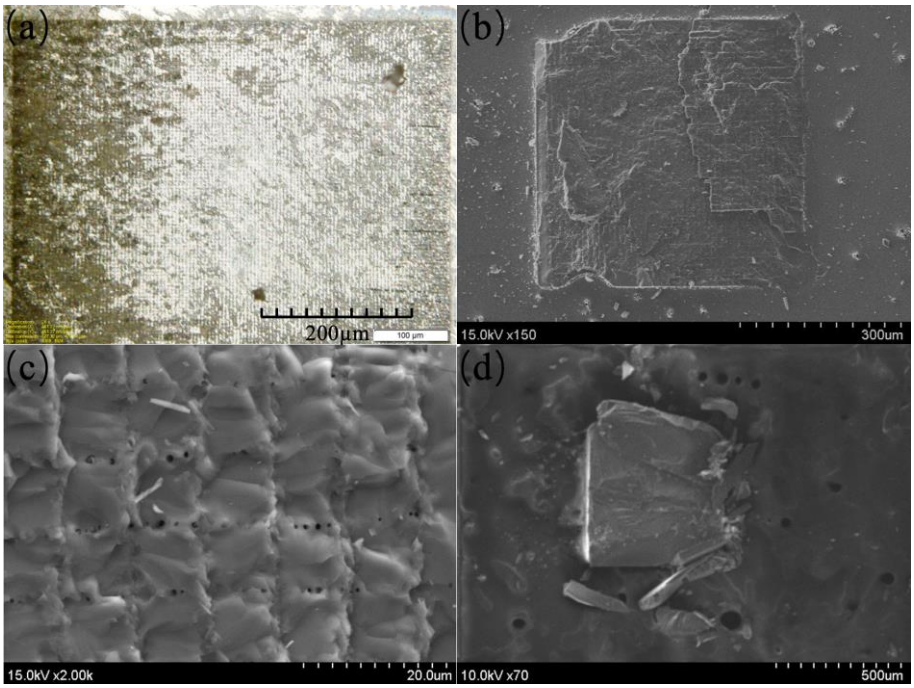

Fig. 8. Microscopic images of (a) smooth silicon surface after laser ablation, (b) substrate after the shear force test, (c) magnified substrate after the shear force test, and (d) the separated layer on top.

3.2 Discussion

The shear stress required to separate the patterns from the substrate was below 200 MPa for most conditions, and it could get to a minimum of 13.1 MPa by increasing the laser power. Typical metal-to-metal bonding shear strength is several ten MPa or higher. Therefore, a shear strength of 13.1 MPa is as a result of the SD layer. On the other hand, this shear strength is still too high to separate the device without damage. Based on the data from the shear force test, shear stress can be reduced by narrowing the laser scanning pitch, increasing laser power, and enlarging the pattern size. It is possible that even a lower shear strength could be obtained by using, for example, a scanning pitch of 5 μm, laser power of 150 and pattern size of 500×500 μm^2. It is also worth mentioning that the laser used in this study was a commercially-available one and different from one used in Disco's stealth dicers, which was specially optimized for stealth dicing. It is expected that using such a special laser can significantly reduce the shear stress for separation. Although it is currently challenging to remove the top layer without causing damage, the results presented here indicate that it is possible. Future work should focus on further optimizing laser ablation parameters to identify the optimal separation conditions. Additionally, the current separation force is limited to shear force; however, applying a combination of forces, including shear, lifting, and torsional forces, could make damage-free separation more easily achievable.

4. Conclusions

The feasibility of using stealth laser dicing along a two-dimensional patterned path was investigated. The test samples consisted of Si substrate with square-shaped structures fabricated by DRIE, that were then ablated by laser stealth dicing following a 2D path and finally separated using a shear stress measurement equipment. The relationships between laser scanning pitch, laser intensity, pattern size, and shear strength have been measured, and the top-view morphology of the SD layer was examined. Lower shear strengths were obtained with smaller scanning pitch, higher laser power and bigger pattern size up to about 20 MPa. The obtained shear strengths, almost all under 200 MPa, suggest that 2D stealth laser dicing could be a viable technique for transferring ultra-thin electronic devices.

References

1) Y. Li, Y. Li, R. Zhang, S. Li, Z. Liu, J. Zhang and Y. Fu, Biosensors and Bioelectronics **237**, 115509 (2023).
2) T. R. Ray, J. Choi, A. J. Bandodkar, S. Krishnan, P. Gutruf, L. Tian, R. Ghaffari and J. A. Rogers, Chem. Rev. **119** [8], 5461 (2019).
3) T. Yokota, K. Fukuda and T. Someya, Advanced Materials **33** [19], 2004416 (2021).
4) M. Lin, Z. Zhang, X. Gao, Y. Bian, R. S. Wu, G. Park, Z. Lou, Z. Zhang, X. Xu, X. Chen, A. Kang, X. Yang, W. Yue, L. Yin, C. Wang, B. Qi, S. Zhou, H. Hu, H. Huang, M. Li, Y. Gu, J. Mu, A. Yang, A. Yaghi, Y. Chen, Y. Lei, C. Lu, R. Wang, J. Wang, S. Xiang, E. B. Kistler, N. Vasconcelos and S. Xu, Nat Biotechnol **42** [3], 448 (2024).
5) H. C. Ko, M. P. Stoykovich, J. Song, V. Malyarchuk, W. M. Choi, C.-J. Yu, J. B. Geddes Iii, J. Xiao, S. Wang, Y. Huang and J. A. Rogers, Nature **454** [7205], 748 (2008).
6) J.-H. Ahn and J. H. Je, J. Phys. D: Appl. Phys. **45** [10], 103001 (2012).
7) K. Huang, R. Dinyari, G. Lanzara, J. Y. Kim, J. Feng, C. Vancura, F.-K. Chang and P. Peumans, in *2007 IEEE International Electron Devices Meeting* (IEEE, Washington, DC, USA, 2007) pp. 217.
8) J. P. Rojas, A. Arevalo, I. G. Foulds and M. M. Hussain, Applied Physics Letters **105** [15], 154101 (2014).
9) W.-L. Sung, W.-C. Lai, C.-C. Chen, K. Huang and W. Fang, in *2014 IEEE 27th International Conference on Micro Electro Mechanical Systems (MEMS)* (IEEE, San Francisco, CA, USA, 2014) pp. 1135.
10) S. V. Joshi, S. Sadeghpour and M. Kraft, in *2023 IEEE 36th International Conference on Micro Electro Mechanical Systems (MEMS)* (IEEE, Munich, Germany, 2023) pp. 331.
11) S. V Joshi, S. Sadeghpour, and M. Kraft, *22nd International Conference on Solid-State Sensors, Actuators and Microsystems (Transducers)*, 2023, pp. 849–852.
12) F. Pavageau, C. Dieppedale, P. Perreau, R. Liechti, A. Hamelin, C. Licitra, F. Casset and G. Le Rhun, Sensors and Actuators A: Physical **346**, 113866 (2022).
13) T. Samoto, H. Hirano, T. Somekawa, K. Hikichi, M. Fujita, M. Esashi and S. Tanaka, J. Micromech. Microeng. **25** [3], 035015 (2015).
14) F. Wang, Q. Liu, J. Xia, M. Huang, X. Wang, W. Dai, G. Zhang, D. Yu, J. Li and R. Sun, Adv Materials Technologies **8** [7], 2201186 (2023).
15) R. Delmdahl, R. Pätzel and J. Brune, Physics Procedia **41**, 241 (2013).
16) R. Delmdahl, M. Fricke and B. Fechner, Journal of Information Display **15** [1], 1 (2014).
17) T. Ueda, M. Ishida and M. Yuri, Jpn. J. Appl. Phys. **50** [4R], 041001 (2011).
18) C.-F. Chu, F.-I. Lai, J.-T. Chu, C.-C. Yu, C.-F. Lin, H.-C. Kuo and S. C. Wang, Journal of Applied Physics **95** [8], 3916 (2004).
19) S.-J. Kim, T. Ahn, M. C. Suh, C.-J. Yu, D.-W. Kim and S.-D. Lee, Jpn. J. Appl. Phys. **44** [8L], L1109 (2005).
20) L. Yue, J. Xu, X. Wang, J. Zhou, Y. Wang, L. Yao, M. Niu, M. Wang, B. Cao, Y. Xu, J. Wang and K. Xu, Jpn. J. Appl. Phys. **63** [5], 051007 (2024).
21) F. Chancerel, P. Urban, J. Slabbekoorn, S. Halas, J. Bravin, S. Brems, T. Uhrmann, M. Wimplinger, A. Phommahaxay and E. Beyne, in *2024 IEEE 74th Electronic Components and Technology Conference (ECTC)* (IEEE, Denver, CO, USA, 2024) pp. 343.
22) "IR LayerRelease™ Technology." Accessed: Nov. 22, 2024.[Online]. Available: https://www.evgroup.com/technologies/ir-layerrelease-technology
23) "レーザーリフトオフ（LLO, Laser Lift-Off）加工", Accessed: Jan. 20, 2024. [Online]. Available: https://technology.disco.co.jp/jp/method/laser-lift-off/
24) "最先端デバイス3次元実装の技術革新に貢献するレーザ剥離技術を開発." Accessed: Jan. 20, 2024. [Online]. Available: https://www.tel.co.jp/news/product/2023/20231211_001.html

25) M. Kumagai, N. Uchiyama, E. Ohmura, R. Sugiura, K. Atsumi and K. Fukumitsu, IEEE Trans. Semicond. Manufact. **20** [3], 259 (2007).
26) M. Fujita, Y. Izawa, Y. Tsurumi, S. Tanaka, H. Fukushi, K. Sueda, Y. Nakata, M. Esashi and N. Miyanaga, IEEJ Trans. SM **130** [4], 118 (2010).
27) Y. Izawa, Y. Tsurumi, S. Tanaka, H. Fukushi, K. Sueda, Y. Nakata, M. Esashi, N. Miyanaga and M. Fujita, IEEJ Trans. SM **129** [3], 63 (2009).
28) M. R. Marks, K. Y. Cheong and Z. Hassan, Precision Engineering **73**, 377 (2022).
29) D. K. Lim, V. R. S. P. Vempaty, A. H. Shah, W. H. Sim and H. V. Singh, IEEE Trans. Compon., Packag. Manufact. Technol. **13** [9], 1486 (2023).
30)W. H. Teh, M.Sc. Thesis, Massachusetts Institute of Technology, Cambridge (2015).
31) L. Wang, C. Zhang, F. Liu, H. Zheng and G. J. Cheng, Journal of Manufacturing Processes **81**, 562 (2022).
32) Y. Yao, A. Vergara, and S. Tanaka, "Feasibility Study of Layer Separation using 2D Patterned Internal Laser Damage in Silicon," in *37th International Microprocesses and Nanotechnology Conference (MNC 2024)*, Kyoto: The Japan Society of Applied Physics, Nov. 2024, 15D-2-3.